

# Speckle Reduction by Phase-based Weighted Least Squares

Lei Zhu<sup>1</sup>, Weiming Wang<sup>2,\*</sup>, Jing Qin<sup>2</sup> and Pheng-Ann Heng<sup>1</sup>

**Abstract**—Although ultrasonography has been widely used in clinical applications, the doctor suffers great difficulties in diagnosis due to the artifacts of ultrasound images, especially the speckle noise. This paper proposes a novel framework for speckle reduction by using a phase-based weighted least squares optimization. The proposed approach can effectively smooth out speckle noise while preserving the features in the image, e.g., edges with different contrasts. To this end, we first employ a local phase-based measure, which is theoretically intensity-invariant, to extract the edge map from the input image. The edge map is then incorporated into the weighted least squares framework to supervise the optimization during despeckling, so that low contrast edges can be retained while the noise has been greatly removed. Experimental results in synthetic and clinical ultrasound images demonstrate that our approach performs better than state-of-the-art methods.

## I. INTRODUCTION

Among many imaging modalities that have been developed for clinical diagnosis and therapy, ultrasonography is the most favorable because it is noninvasive, real-time and easy to operate. Unfortunately, ultrasound images are inevitably corrupted by speckle noise, which increases the difficulties of processing and analysis on these images. It is thus essential and meaningful to remove the speckle from ultrasound images so as to simplify their usages in clinical applications.

A lot of approaches have been proposed for speckle reduction. Both Lee filter [1] and Frost filter [2] update the intensity for each pixel by weighting the pixels inside the filter window based on local coefficient variance. Later, Lopes et al. [3] enhanced these filters by first classifying all the pixels into three clusters and then applying specific processing on each cluster. Moreover, the squeeze box filter [4] removes local extrema that are assumed to be outliers by replacing them with local means.

Some edge-preserving smoothing operators designed for natural images have been extended for speckled images. Yu and Acton [5] proposed an edge-sensitive approach to reduce speckle based on anisotropic diffusion [6] that encourages intraregion smoothing in preference to interregion smoothing. Krissian et al. [7] further proposed an oriented speckle reducing anisotropic diffusion by considering local directional variance of the image intensity. These approaches can gradually smooth the speckled image. However, a lot

of meaningful details are discarded and the despeckled result usually converges to a constant-value image. Bilateral filter [8][9] is originally proposed to remove additive noise by weighting the spatial and the range distances between two neighboring pixels. Based on this, Balocco et al. [10] presented a speckle reducing bilateral filter by embedding the noise statistics in the weighting scheme. Non-local means (NLM) filter [11] has also been utilized to remove speckle noise, and Couple et al. [12] employed the Bayesian framework to derive a NLM filter that adapts to ultrasound data by defining a Pearson distance for the speckle model.

Wavelet-based methods are also exploited for speckle reduction. Yue et al. [13] described a nonlinear multiscale wavelet diffusion approach for noise suppression. It makes use of the sparsity and multiresolution properties of the wavelets and the edge enhancement feature of nonlinear diffusion. Recently, Esakkirajan et al. [14] presented an adaptive wavelet packet-based smoothing approach by combining the bilateral filter. However, these methods tend to produce ringing artifacts due to the multiresolution and directionality characteristics of wavelet transformation.

The goals of speckle reduction are two manifolds. On one hand, we want to smooth the speckled image as much as possible except across significant features, e.g., object boundaries. On the other hand, the despeckled image shall be as close as possible to the original one so that important structures are not damaged. In this paper, we propose a novel approach to achieve these goals based on the weighted least squares (WLS) framework [15]. WLS has been shown to have the nice property of smoothing image details at different scales without blurring the features. However, we demonstrate that the original gradient-based WLS is not suitable for ultrasound images while its phase-based counterpart turns out to be a better alternative as phase-based methods are robust to noise and attenuation artifacts. Based on this observation, we employ a local phase-based measure to extract the edge map from the speckled image. The edge map is then incorporated into the WLS framework as a weighting function to supervise the optimization during despeckling. Attributing to the intensity-invariant property of the phase-based measure, we can effectively remove speckle noise while preserving the edges in the image.

## II. METHOD

### A. Multiscale Feature Asymmetry

Local energy model developed in [16] postulates that features are perceived at points where the Fourier components are maximally in phase. In [17], Felsberg et al. proposed a 2D

<sup>1</sup>Lei Zhu and Pheng-Ann Heng are with Department of Computer Science and Engineering, The Chinese University of Hong Kong, Shatin N.T. Hong Kong.

<sup>2</sup>Weiming Wang and Jing Qin are with Center for Human Computer Interaction, Shenzhen institutes of Advanced Technology, Chinese Academy of Sciences, Shenzhen China.

\*Corresponding author: wm.wang@siat.ac.cn.

isotropic analytic signal, called monogenic signal, to perform local analysis. The monogenic signal is defined by combining the original 2D signal  $f$  with its Riesz transform  $f_R$  to form a 3D vector  $f_M = (f, f_R) = (f, r_1 * f, r_2 * f)$ , where  $r_1$  and  $r_2$  are the Riesz filters. In practice, local analysis is usually performed via a bank of bandpass quadrature filters tuned to various spatial frequencies because real images generally consist of a wide range of frequencies. Therefore, a set of bandpass filters  $g$  are combined with the monogenic signal, which now becomes:  $f_M = (g * f, g * r_1 * f, g * r_2 * f) = (even, odd)$ , where *even* and *odd* represent the scalar-valued even and the vector-valued odd responses of the quadrature filters, respectively. As suggested in [18], we choose Cauchy kernels as bandpass filters due to their nice property of localization. In frequency domain, a 2D isotropic Cauchy kernel is defined as

$$G(\omega) = n_c |\omega|^a \exp(-s|\omega|), \quad (1)$$

where  $a \geq 1$ ,  $\omega = (u, v)$ ,  $s$  is the scale parameter and  $n_c$  is a normalization constant. Please refer to [18] for more details about the parameters.

In [19], Kovesi pointed out that, at points of asymmetry, the absolute values of odd symmetric filter responses are large while the absolute values of even symmetric filter responses are small, and suggested to use the differences between the odd and the even symmetric filter responses over a number of scales to detect step edge-like features. In light of this, we define a multiscale feature asymmetry measure to extract the edges from ultrasound images as

$$MSFA = \frac{\sum_n [|\text{odd}_n| - |\text{even}_n| - T_n]}{\sum_n \sqrt{\text{odd}_n^2 + \text{even}_n^2 + \varepsilon}}, \quad (2)$$

where  $\varepsilon$  is a small constant to avoid division by zero;  $T_n$  is the scale specific noise threshold and  $[\cdot]$  denotes the zeroing of negative values. The MSFA measure takes values between 0 and 1, close to 0 in smooth regions and close to 1 near the boundaries.

Phase-based measures have been successfully used for edge detection in ultrasound images [20][21] because of their invariance to variations in image contrast. Our MSFA measure shares the same property, as shown in Fig. 1. Note that the boundary contrast of the inner object is much lower than the one of the outer object. Nevertheless, the MSFA edge map precisely captures the boundaries of the two circular objects. In contrast, the responses in the gradient edge map are rather weak since it is directly related to the intensity of the image. The situation is even worse in low contrast regions and the boundaries of the inner object is almost invisible in the gradient edge map.

### B. Phase-based Weighted Least Squares

As stated previously, to remove speckle noise from an ultrasound image  $S$ , we seek to find a new image  $I$ , which is as close as possible to  $S$  but is also as smooth as possible everywhere, except across significant features. The weighted

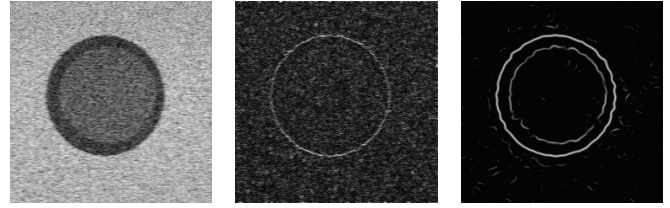


Fig. 1. Edge detection in a synthetic ultrasound image. (Left) Input image. (Middle) Gradient edge map. (Right) MSFA edge map.

least squares framework formulates the balance of those two goals by minimizing the following energy function

$$\sum_p \left( (S_p - I_p)^2 + \lambda \left( w_{x,p}(S) \left( \frac{\partial I}{\partial x} \right)_p^2 + w_{y,p}(S) \left( \frac{\partial I}{\partial y} \right)_p^2 \right) \right) \quad (3)$$

where  $p$  is the pixel location and  $\lambda$  balances the impact between the two parts of the energy function. The first part corresponds to the data term that is used to minimize the difference between  $S$  and  $I$ . The second part contains two partial derivatives, which are used to smooth the resultant image.  $w_{x,p}(S)$  and  $w_{y,p}(S)$  are two weighting functions and are typically set to be identical [15].

Unfortunately, traditional WLS does not work well when directly applied to ultrasound images because of the characteristic artifacts. One major reason is that the weighting functions are usually defined based on image gradient, which is rather weak for ultrasound data. We solve this problem by combining the above MSFA measure and the WLS optimization into a unified framework. Specifically, we develop a phase-based WLS framework by setting the two weighting functions with the MSFA measure as

$$w_{x,p}(S) = w_{y,p}(S) = ((MSFA_p(S))^\alpha + \varepsilon)^{-1} \quad (4)$$

where  $\alpha$  controls the sensitivity of the MSFA edge map. Eq. 4 plays an important role in adapting WLS to ultrasound images. Different from gradient-based operators, the MSFA measure is robust to noise and attenuation artifacts, and it only responds high to the edges in the images. Therefore, the values of the weighting function are quite low at the edges, which prohibited image smoothing. In contrast, smoothing is greatly encouraged in homogeneous regions, resulting in edge-preserving speckle reduction.

In order to minimize Eq. 3, we rewrite it into the following matrix form

$$(S - I)^T (S - I) + \lambda (S^T C_x^T W_x C_x S + S^T C_y^T W_y C_y S) \quad (5)$$

where matrices  $C_x$  and  $C_y$  are discrete differentiation operators.  $W_x$  and  $W_y$  are diagonal matrices, and their values are set as  $W_x[i, i] = w_{x,p}(S)$  and  $W_y[i, i] = w_{y,p}(S)$ . Finally, minimization of Eq. 3 boils down to solving the following linear system

$$(A + \lambda L)S = I \quad (6)$$

where  $A$  is the identity matrix and  $L = C_x^T W_x C_x + C_y^T W_y C_y$ .

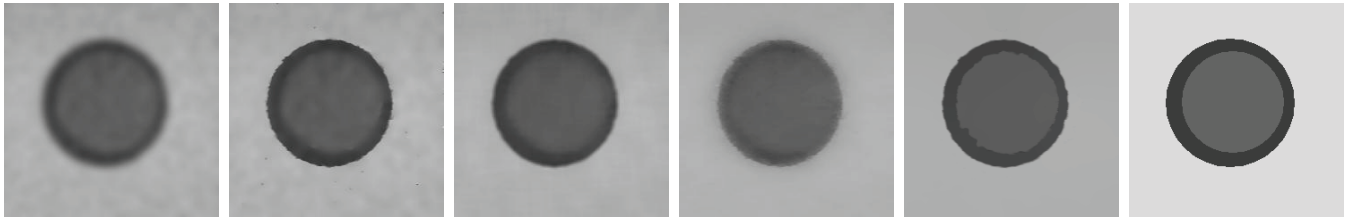


Fig. 2. Comparison of speckle reduction with a synthetic ultrasound image (left of Fig. 1). From left to right: Lee's result [1], Yu's result [5], Coupé's result [12], Farbman's result [15], our result and the ground truth.

### III. EXPERIMENTS

In this section, we validate the performance of the proposed approach with both synthetic and clinical ultrasound images. To demonstrate the advantages of our approach, several state-of-the-art methods are also executed for comparison. For all the methods, we use the parameters that produce the best results. We also adopt two widely used measures to quantitatively evaluate the performance of these methods: Pratt's figure of merit (FOM) and mean structural similarity (MSSIM). FOM is mainly used to assess the accuracy of edge preservation and is defined as

$$FOM = \frac{1}{\max\{\hat{N}, N_{ideal}\}} \sum_{i=1}^{\hat{N}} \frac{1}{1 + d_i^2 \beta} \quad (7)$$

where  $\hat{N}$  and  $N_{ideal}$  are the number of detected and ideal edge pixels, respectively.  $d_i$  is the Euclidean distance between the  $i$ th edge pixel and the nearest ideal edge pixel, and  $\beta$  is a constant that is usually set to be 1/9. The values of FOM vary from 0 to 1, and larger values indicate a better performance on edge preservation. MSSIM is generally used to assess the similarity between two images  $S_1$  and  $S_2$ , and is computed as

$$MSSIM(S_1, S_2) = \frac{1}{N} \sum_{i=1}^N SSIM((S_1)_i, (S_2)_i) \quad (8)$$

where  $N$  is the number of pixels in  $S_1$  or  $S_2$ , and SSIM [22] is defined as

$$SSIM(S_1, S_2) = [l(S_1, S_2)]^{\gamma_1} \times [C(S_1, S_2)]^{\gamma_2} \times [S(S_1, S_2)]^{\gamma_3} \quad (9)$$

where  $l(S_1, S_2)$ ,  $C(S_1, S_2)$  and  $S(S_1, S_2)$  are three functions to compute the differences of luminance, contrast and structure between  $S_1$  and  $S_2$ , respectively. The parameters  $\alpha$ ,  $\beta$  and  $\gamma$  are used to adjust the importance of each function. The values of MSSIM are also between 0 and 1, and higher values means less difference between the two images.

#### A. Synthetic Images

The phantom data is synthesized using the simulation program Field II [23], see left of Fig. 1. There are two circular objects in the foreground. The contrast between the background and the outer object is relatively high while the contrast between the outer and the inner objects is relatively low. Fig. 2 shows the despeckled images of five methods. As can be seen, the first four methods tend to

TABLE I

COMPARISON OF FOM AND MSSIM MEASUREMENTS OF THE FIVE METHODS IN THE SYNTHETIC ULTRASOUND IMAGE (LEFT OF FIG. 1).

	Lee's method	Yu's method	Coupé's method	Farbman's method	Our method
FOM	0.2888	0.4578	0.5855	0.3023	0.8286
MSSIM	0.7435	0.7698	0.7909	0.7483	0.8954

smooth the object boundaries in order to remove the speckle noise. The situation is even severer in low contrast regions where the boundaries of the inner object is heavily blurred. In contrast, our approach perfectly smooths homogeneous regions and preserves the boundaries of the two objects. Tab. I lists the FOM and MSSIM measurements of the five methods. Our approach achieves the highest value in the two measurements, which means that our result is the most similar to the ground truth.

#### B. Clinical Images

Fig. 3 shows the results of speckle reduction in a left ventricle and a breast tumor ultrasound images. Again, our approach greatly remove the speckle noise while the edges of important structures are still preserved. Four other methods are also presented for comparison. For these methods, the price paid for smoothing the speckled images if the blurring of the edges. One interesting thing is about the original WLS model [15]. As shown in the figures, near blurred edges, this model cannot correctly classify pixels into homogeneous regions, leading to even more blurred of the edges. Our approach precisely captures the object boundaries, and then encourages intraregion smoothing while prevent interregion smoothing so as to preserve the edges. This is attributed to the intensity-invariant property of the local phase-based measure, where both high and low contrast edges can be accurately located. All the experiments demonstrate the feasibility and superiority of the phase-based WLS.

### IV. CONCLUSION

In this paper, we propose a novel phase-based framework to reduce speckle noise in ultrasound images. Different from previous methods, our approach can greatly remove the speckle but effectively preserve low contrast features in the image. This is achieved by combining the MSFA measure and the WLS optimization into a unified framework. The MSFA measure is independent to image intensity and can

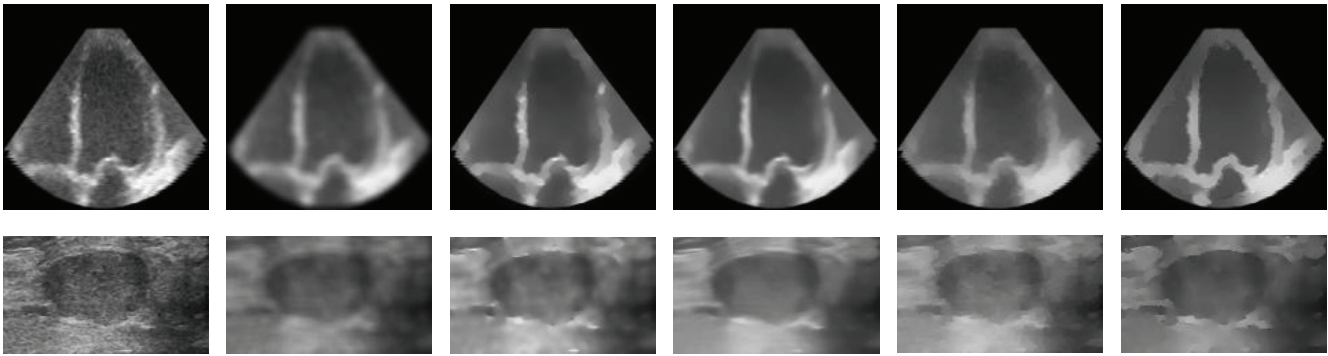


Fig. 3. Comparison of speckle reduction with a left ventricle (Top) and a breast tumor (Bottom) ultrasound images. From left to right: input images, Lee's results [1], Yu's results [5], Coupé's results [12], Farberman's results [15] and our results.

accurately extract the edge map from low contrast ultrasound images. The MSFA edge map enables WLS with the ability of edge-sensitive during despeckling. Experimental results demonstrate the advantages of the proposed approach in comparison with state-of-the-art methods.

There are also some limitations about our approach. Like other feature detection methods, the MSFA measure cannot fully capture the features in the image due to the limited number of scales used in the detection computation. The features that are missed in the feature map will not be preserved after smoothing. In addition, some noise may be identified as image features by the MSFA measure and larger  $\lambda$  is required in order to smooth out these false features, which will result in certain degree of blurring of the image. In future work, we will try to solve these problems by optimizing the performance of the phase-based measure.

#### ACKNOWLEDGMENT

The work described in this paper was partially supported by a grant from the Hong Kong Innovation and Technology Fund (Project No.: GHP/003/11SZ), a grant from Ministry of Science and Technology of the People's Republic of China under the Singapore-China 9th Joint Research Programme (Project No.: 2013DFG12900), and a grant from Natural Science Foundation of Guangdong (Project No.: S2013010014073).

#### REFERENCES

- [1] Jong-Sen Lee. Digital image enhancement and noise filtering by use of local statistics. *IEEE Trans. Pattern Anal. Mach. Intell.*, (2):165–168, 1980.
- [2] Victor S. Frost, Josephine Abbott Stiles, K. Sam Shanmugan, and Julian C. Holtzman. A model for radar images and its application to adaptive digital filtering of multiplicative noise. *IEEE Trans. Pattern Anal. Mach. Intell.*, 4(2):157–166, 1982.
- [3] Armand Lopes, Ridha Touzi, and E Nezry. Adaptive speckle filters and scene heterogeneity. *IEEE Transactions on Geoscience and Remote Sensing.*, 28(6):992–1000, 1990.
- [4] Peter C Tay, Christopher D Garson, Scott T Acton, and John A Hossack. Ultrasound despeckling for contrast enhancement. *IEEE Transactions on Image Processing*, 19(7):1847–1860, 2010.
- [5] Yongjian Yu and Scott T. Acton. Speckle reducing anisotropic diffusion. *IEEE Trans. on Image Processing*, 11(11):1260–1270, 2002.
- [6] Pietro Perona and Jitendra Malik. Scale-space and edge detection using anisotropic diffusion. *IEEE Trans. Pattern Anal. Mach. Intell.*, 12(7):629–639, 1990.
- [7] Karl Krissian, C-F Westin, Ron Kikinis, and Kirby G Vosburgh. Oriented speckle reducing anisotropic diffusion. *IEEE Transactions on Image Processing*, 16(5):1412–1424, 2007.
- [8] Carlo Tomasi and Roberto Manduchi. Bilateral filtering for gray and color images. In *ICCV*, pages 839–846, 1998.
- [9] Lei Zhu, Mingqiang Wei, Jinze Yu, Weiming Wang, Jing Qin, and Pheng-Ann Heng. Coarse-to-fine normal filtering for feature-preserving mesh denoising based on isotropic subneighborhoods. *Comput. Graph. Forum*, 32(7):371–380, 2013.
- [10] Simone Balocco, Carlo Gatta, Oriol Pujol, Josepa Mauri, and Petia Radeva. Sbrf: Speckle reducing bilateral filtering. *Ultrasound in medicine & biology*, 36(8):1353–1363, 2010.
- [11] Antoni Buades, Bartomeu Coll, and Jean-Michel Morel. A non-local algorithm for image denoising. In *CVPR (2)*, pages 60–65, 2005.
- [12] Pierrick Coupé, Pierre Hellier, Charles Kervrann, and Christian Barillot. Nonlocal means-based speckle filtering for ultrasound images. *IEEE Transactions on Image Processing*, 18(10):2221–2229, 2009.
- [13] Yong Yue, Mihai M Croitoru, Akhil Bidani, Joseph B Zwischenberger, and John W Clark. Nonlinear multiscale wavelet diffusion for speckle suppression and edge enhancement in ultrasound images. *IEEE Trans. Med. Imaging*, 25(3):297–311, 2006.
- [14] Sankaralingam Esakkirajan, Chinna Thambi Vimalraj, Rashad Muhammed, and Ganapathi Subramanian. Adaptive wavelet packet-based de-speckling of ultrasound images with bilateral filter. *Ultrasound in medicine & biology*, 39(12):2463–2476, 2013.
- [15] Zeev Farberman, Raanan Fattal, Dani Lischinski, and Richard Szeliski. Edge-preserving decompositions for multi-scale tone and detail manipulation. *ACM Trans. Graph.*, 27(3), 2008.
- [16] M. C. Morrone, J. Ross, D. C. Burr, and R. Owens. Mach bands are phase dependent. *Nature*, 324(6094):250–253, 1986.
- [17] Michael Felsberg and Gerald Sommer. The monogenic signal. *IEEE Transactions on Signal Processing*, 49(12):3136–3144, 2001.
- [18] Djamel Boukerroui, J. Alison Noble, and Michael Brady. On the choice of band-pass quadrature filters. *Journal of Mathematical Imaging and Vision*, 21(1-2):53–80, 2004.
- [19] Peter Kovsi. Symmetry and asymmetry from local phase. In *Tenth Australian joint conference on artificial intelligence*, volume 190. Citeseer, 1997.
- [20] Ahror Belaid, Djamel Boukerroui, Yves Maingourd, and Jean-François Lerallut. Phase-based level set segmentation of ultrasound images. *IEEE Transactions on Information Technology in Biomedicine*, 15(1):138–147, 2011.
- [21] Weiming Wang, Jing Qin, Lei Zhu, Dong Ni, Yim-Pan Chui, and Pheng-Ann Heng. Detection and measurement of fetal abdominal contour in ultrasound images via local phase information and iterative randomized hough transform. *Bio-Medical Materials and Engineering*, 24(1):1261–1267, 2014.
- [22] Zhou Wang, Alan C Bovik, Hamid R Sheikh, and Eero P Simoncelli. Image quality assessment: from error visibility to structural similarity. *IEEE Transactions on Image Processing*, 13(4):600–612, 2004.
- [23] Jørgen Arendt Jensen. Field: A program for simulating ultrasound systems. In *Proc. 10th Nordic-Baltic Conf. Biomed. Imag.*, volume 34, pages 351–353, 1996.